(2)

Journal Name

ARTICLE TYPE

Cite this: DOI: 00.0000/xxxxxxxxxx

Phase stability in nickel phosphides at high pressures

Talgat M. Inerbaev,*[ab] Nursultan Sagatov,[ac], Dinara Sagatova,[ac] Pavel N. Gavryushkin,[ac] Abdirash T. Akilbekov,[b] and Konstantin D. Litasov[de]

Received Date
Accepted Date

DOI: 00.0000/xxxxxxxxxx

Phosphorus – one of the light elements of the Earth's core and planets. High-pressure behaviour of phosphporus compounds with nickel and iron attract considerable attention due to their findings in meteorites and xenolites (поправьте меня, если я не прав) In the present work with modern methods of crystal structure prediction we investigate structures and stability of compounds in Ni-P systems at pressures of 100-400 GPs. As the result the series of (Ni,P) solid solutions, presents by compounds $Ni_{14}P$, $Ni_{12}P$, $Ni_{10}P$, Ni_8P, Ni_7P, Ni_5P, Ni_3P, is revealed. Phosphorus show sufficient solubility in *fcc* structure of Ni, and up to 25 mol.% of this element can be dissolved at low temperatures. Based on the comparison of compounds in Ni-P and Fe-P systems we suggest, that Ni facilitate phosphorus dissolution in closed-packed structure of *d*-metal, and dissolution of P in (Ni,P) alloy is higher, than in pure Fe. For the phosphide of the Ni_3P composition, a new high-pressure phase of the *Cmca* space group is predicted. This structure can be described as defromed *fcc* packing, The transition from the low-pressure phase of Ni_3P-$I\bar{4}$ to the *Cmca* phase occurs at a pressure of 62 GPa, regardless of the external temperature. Ni_2P is stabilised at pressure above 200 GPa in the form of allabogdanite structure. The transition from barringerite to allabogdanite is predicted to occur in the range of 78–88 GPa at temperatures 0-2000 K.

1 Introduction

Phosphides play a significant role in the mineralogy of iron meteorites as a component of the ternary Fe-Ni-P system. Although being rare, accessory minerals with composition $(Fe,Ni)_xP$, gives important information about phosphourus geochemistry on the early stages of the universe formation.[1–10] The occurrence of these minerals in meteoritic samples is believed to originate either from the equilibrium condensation of protoplanetary materials taking place in solar nebulae or from crystallization processes in the cores of parent bodies.

Fe end-members were intensively studied using both experimental and theoretical techniques. So far, most of the high-pressure investigations on iron phosphides have been restricted on Fe_4P,[11] Fe_3P,[12] Fe_2P[13,14] and FeP.[15] Several structural and magnetic phase transitions have been revealed as the result. Dera et al. observed that on heating at 8 GPa phase of Fe_2P transforms to a high-pressure modification, which could be quenched to ambient conditions.[13] Theoretical modelling demonstrates that the stable phase of Fe_2P should be the *Pnma* with the lowest total energy at lower pressure, and the $P\bar{6}2m$ and *Pnma* phases would transform to the $P\bar{3}m$ phase with larger coordination number of iron at 125 GPa and 153 GPa, respectively.[14] Theoretical studies have shown that Fe_3P could decompose into Fe_2P and Fe_4P at pressures higher than 214 GPa [16], and Fe_3P and Fe would react with formation of Fe_4P at ~100 GPa.[11] Fe_3P exhibits a structural phase transition from $I4$ to $P4/mnc$ at 64 GPa and 1600 K accompanied with an electronic state transition from high spin to low spin at around 20-40 GPa.[17,18] Upon compression, Fe_4P undergoes transition from ferromagnetic to nonmagnetic state at 80 GPa.[11] Britvin et al. reported two new structures of FeP (*Pnma*) and FeP_2 (*Pnnm*), found in the pyrometamorphic rocks.[8,9]

Alloying effect of Ni on physical properties and structure of Fe and it's alloys with light elements is also of geological interest, as according to geochemical assesment Earth's core could contain up to 10mol% of Ni (Уточнить и поставить ссылку на Чёрную Книжку (?)). Addition of nickel to iron phosphides affect the structure and phase stability. The example of Fe_2P shows, that a small addition of Ni and Co stabilise the structure of alabogdanite against ... [3,4,19], and also slightly increases

[a] Sobolev Institute of Geology and Mineralogy, Siberian Branch of the Russian Academy of Sciences, Novosibirsk, 630090 Russia. E-mail: inerbaevtm@igm.nsc.ru
[b] L. N. Gumilyov Eurasian National University, Nur-Sultan, 010008 Kazakhstan.
[c] Novosibirsk State University, Novosibirsk, 630090 Russia.
[d] Vereshchagin Institute for High Pressure Physics, Russian Academy of Sciences, Moscow, 108840, Russia.
[e] Fersman Mineralogical Museum Russian Academy of Sciences, Moscow, Russia.

Table 1 Structural data for the predicted phases of Ni–P system –(1) Здесь необходимо привести данные предсказанного аллабогданита-Ni_2P, чтобы желающие могли убедиться что это действительно аллабогданит. Параметры ячейки могут пригодиться экспериментаторам для расшифровки дифрактограмм. Вообщем привести стоит. – (2) Параметры ячейки лучше округлить до тысячных, четвёртая цифра абсолютно не значима. Координаты атомов – до десятитысячных (именно так делает большинство авторов, например К. Пикард, лично я бы всё до тысячных округлял))

Phase	Pressure (GPa)	Space group	Lattice parameters (Å, degree)			Atomic coordinates			
						Atom	x	y	z
$Ni_{14}P$	400	$C2/m$ (#12)	a=6.8686Å	b=6.2097Å	c=5.0749Å	Ni1	0.00000	0.16860	0.00000
			α=90	β=119.559	γ=90	Ni2	0.09850	0.00000	0.39699
						Ni3	0.30065	0.00000	0.19837
						Ni4	0.70280	0.33474	0.80023
						Ni5	0.59887	0.16587	0.39807
						P1	0.00000	0.50000	0.00000
$Ni_{12}P$	400	$R\bar{3}$(#148)	a=7.4609Å	b=7.4609Å	c=5.0755Å	Ni1	0.53902	0.38422	0.00134
			α=90.00	β=90.00	γ=120	Ni2	-0.02851	0.40876	0.33153
						P1	0.00000	0.00000	0.00000
$Ni_{10}P$	300	$P\bar{1}$ (#2)	a=3.6654Å	b=4.7295Å	c=4.7339Å	Ni1	0.04502	0.41007	0.18032
			α=107.482	β=104.937	γ=97.456	Ni2	0.59015	0.31912	0.35915
						Ni3	0.13716	0.22851	0.54678
						Ni4	0.22672	0.04944	-0.09103
						Ni5	0.67759	0.13805	0.72806
						P1	0.50000	0.50000	0.00000
Ni_8P	200	$P\bar{1}$ (#2)	a=3.7669Å	b=3.7719Å	c=4.8694Å	Ni1	0.22148	0.11048	0.56082
			α=75.00	β=82.569	γ=80.481	Ni2	0.67093	0.33311	0.66740
						Ni3	0.44401	0.21845	0.11085
						Ni4	0.11116	0.55650	0.78047
						P1	0.00000	0.00000	0.00000
Ni_7P	100	$P\bar{1}$ (#2)	a=3.7553Å	b=3.7772Å	c=4.3925Å	Ni1	0.50201	0.00029	0.24766
			α=73.032	β=89.980	γ=79.849	Ni2	0.00000	0.00000	0.50000
						Ni3	0.75389	0.49840	0.12435
						Ni4	0.24895	0.50693	0.37130
						P1	0.00000	0.00000	0.00000
Ni_5P	200	$P6_3/mcm$ (#193)	a=3.7732Å	b=3.7732Å	c=7.0786Å	Ni1	0.33333	0.66667	0.00000
			α=90.00	β=90.00	γ=120	Ni2	0.67096	0.00000	0.25000
						P1	0.00000	0.00000	0.00000
Ni_3P	100	$Cmca$ (#64)	a=13.1666Å	b=4.4854Å	c=4.4851Å	Ni1	0.38137	0.00000	0.00000
			α=90.00	β=90.00	γ=90.00	Ni2	0.00000	0.18176	0.81801
						Ni3	0.25000	0.74729	0.25000
						P1	0.13651	0.00000	0.00000

the bulk modulus of the allabogdanite phase.[19] А может здесь сослаться на нашу статью по алабогданиту (Bekker, Sagatov et al., 2020)? The incorporation of Ni in nonmagnetic Fe_4P results in reduction of the compressional and shear wave velocities enhancing their anisotropy.[11]

There are numerous phases were revealed in Ni–P system at ambient pressure. Among them are Ni_3P, Ni_8P_3, $Ni_{12}P_5$, Ni_2P, Ni_5P_4, NiP, NiP_2, and NiP_3. However, the data on this system at high-pressures, especially above 100 GPa, are limited. Donohue et al.[20] studied P-rich compositions ($NiP_{2.2-2.5}$) at 1.5-6.5 GPa. Dera et. al.[21] synthesized a cubic NiP_2 phase at 6.5 GPa during heating at 1200°C and subsequent cooling to 900°C. Incongruent melting associated with formation of pyrite-type NiP_2 and amorphous Ni-P alloy was found at an intermediate pressure range, between 6.5 and 40 GPa. The phase transitions in Ni_2P were not observed in these experiments at pressures up to 50 GPa consistently with theoretical modelling.[19] Several reversible phase transitions were established in NiP at ambient temperature: (a) from $Pbca$ to $Cmc2_1$ at 3.5 GPa, (b) to $Pnma$-phase at 8.5 GPa and again to $Cmc2_1$-phase, but with different crystal structure at 25 GPa.[22,23] Litasov et.al. studied the melting processes and subsolidus phase relations in the Ni-Ni_2P system at 6 GPa and 900-1600°C.[24] Хорошо бы в этой и других подобных ссылках отметить конкретный результат. А так получается просто констатация факта, что кто-то что-то исследовал. А что получено в результате? The stability of four intermediate compositions, Ni_3P, Ni_8P_3/Ni_5P_2, $Ni_{12}P_5$, and Ni_2P transjordanite was found. The $Ni_{12}P_5$ phase becomes unstable at 900°C and decomposes into Ni_5P_2 and Ni_2P.

The phase stability, elastic properties, hardness and related electronic structures of Ni–P crystal phases at ambient pressure and zero temperature were studied theoretically in Ref.[25,26]. The equations of state and structural parameters of Ni_2P, NiP_2 (pyrite type) and Ni-doped Fe_2P (allabogdanite) at high pressures were determined with first-principles calculations.[19] There was not found barringerite-allabogdanite phase transition in Ni_2P at pressures up to 50 GPa. Bulk modulus of $(Fe_{1-x}Ni_x)_2P$ (allabogdanite) increases with Ni concentration. Increasing the concentration of Ni decreases the stability of structure and suppresses the total magnetic moment of the system.

In present research, we theoretically investigate Ni-P compounds in the pressure range from 100 to 400 GPa. A search for

new crystalline structures is carried out. The relative stability of all predicted and well-known experimentally observed structures of the Ni–P system is investigated. The phase diagram of the Ni_2P system is calculated, where barringerite-allobogdanite structural phase transition occurs at pressures of 77-87 GPa depending on temperature. Similar calculations of the phase equilibrium between the new high-pressure Ni_3P phase and the schreibersite structure are also performed.

2 Computation Details

The structure predictions were performed using USPEX code based on evolutionary algorithms[27–29] and AIRSS based on a random sampling method.[30,31] Crystal structure prediction calculations were divided into two stages. At the first stage, the search for stable structures of intermediate compositions was performed using the USPEX package. At the second stage, the predictions were performed for the fixed compositions represented on the convex hull constructed at the first stage using USPEX and AIRSS. The calculations of the electronic structure were carried out within the DFT using the VASP 5.4 package.[32,33] The exchange-correlation interaction was taken into account in the generalized gradient approximation (GGA) in the form of the Perdew-Burke-Ernzerhof (PBE) functional[34] in a plane-wave basis set along with projector augmented-wave (PAW) pseudopotentials.[35] For all studied structures, calculations were performed, taking into account the spin polarization. It was found that in all cases, except for the new predicted phases $Ni_{10}P$, $Ni_{12}P$, and $Ni_{14}P$, the magnetic moment is equal to zero. The computation parameters were as follows: energy cut-off – 450 eV; the density of the grid of Monkhorst-Pack k-point mesh – $0.5Å^{-1}$. The most promising predicted structures were then optimized with higher accuracy at various pressures. In these calculations, the cut-off energy was 700 eV and the density of k-points was $0.2Å^{-1}$.

To take into account the temperature effect and predict the phase diagrams, we used the method of lattice dynamics within the quasi-harmonic approximation (QHA). For this task, the phonon frequencies were calculated with the PHONOPY code.[36]

3 Results and Discussion

3.1 The analysis of HP crystal structures

Structural data of the new phases predicted with USPEX and AIRSS codes are summarized in Table 1 and shown in Fig. 1. All found structures are dynamically stable,the corresponding phonon spectra presented in Supporting Information (SI).

The structures of $Ni_{14}P$, $Ni_{12}P$, $Ni_{10}P$, Ni_8P, Ni_7P, Ni_5P, and Ni_3P are characterized by *fcc* packing, witi Ni atoms partially substituted by P atoms. The pure Ni also present in the *fcc* form up to 400 GPa. Thus, the found structures can be considered as (Ni,P) solid solutions. This type of isomorphism between *d*-metal and light element is unusual at ambient pressures. At extreme pressures of the Earth's core, when elements which are typical non-metals like sulphur adopt metallic properties[37], this isomorphism became typical. Isomorphic replacement of iron

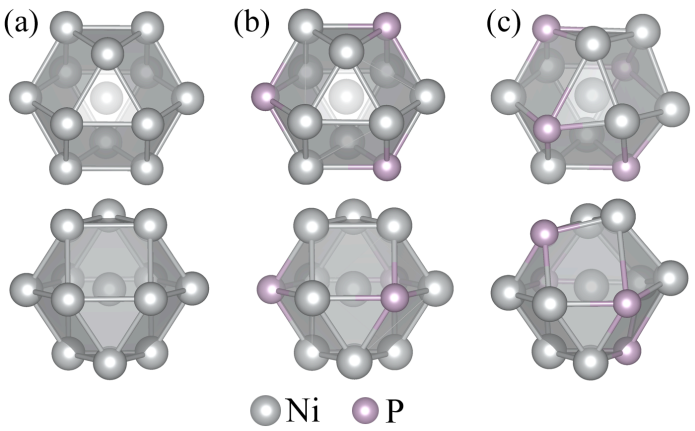

Fig. 1 Coordination cube-octahedron around Ni atoms in fcc-Ni (a), Ni_5P-$P6_3/mcm$ (b), and Ni_3P-*Cmca* (c) structures; upper row – view along three-fold axis, lower row – perpendicular to the three-fold axis – (1) Добавить структуру аллабогданита под буквой (d). – (2) Для имеющихся структур оставить только одну проекцию вдоль оси третьего порядка, слегка наклонённую.

on sulphur within *hcp* or *bcc* crystal structures can be given as exmaple[38]. Я здесь в обоих случаях на себя ссылаюсь, хорошо бы добавить и другие ссылки (например на Cote и Vocadlo), но сходу ничего предложить не могу. Typical for solid solutions, P atoms in found structures tend to be homogenically spread through the structure, without clustering or group formation.

The deformation of the ideal cubic *fcc* structure increases with increasing amount of phosphourus. The deformation of coordination cube-octahedron of ligand Ni and P atoms around central Ni atom can be traced by the changes of Ni-P and Ni-N bond lengths, shown in Supporting information Figure ??. $Ni_{14}P$, $Ni_{12}P$, $Ni_{10}P$, Ni_8P, Ni_7P, Ni_5P structures are characterised by almost ideal fcc packing, with both Ni-Ni and Ni-P bonds of the same length, equal to 2.7 Å at 100 GPa. The Ni-Ni bond in the pure *fcc* Ni is characterised by the same length. Ni_3P structure is sufficiently deformed, as shown on Figure 1, the Ni-P bond is equal to 2.25 Å while length of Ni-Ni bonds vary in the range 2.25-2.35Å. The found Ni_2P-*Pnma* structure is the analogue of allabogdanite mineral with composition Fe_2P. Allabogdanite is of cottunite-type, does not having close-packing of atoms, in contrast to *fcc* structure which is 3-layered close-packing. The calculations, which results will be presented below, show that experimentally synthesises at ambient pressure Ni_8P_3 structure is also stable up to 400 GPa. As well as Ni_2P, the structure of this phase are also not of closed packing type. Thus, around 25 mol.% of P can be dissolved in *fcc* structure of Ni, without heating. As temperature increases the limits of isomorphism, this value can be accepted as the lower boundary for (Ni,P) isomorphism at conditions of the cores of the Earth or planets. The fact, that similar isomorphism was not found in Fe–P systems, likely shows that solubility of P in (Fe,Ni) alloy will be higher than in the pure Fe.

Spin-polarized calculations show the presence of a magnetic moment in structures with a relatively high nickel content from

Ni_{14} to Ni_8P, as shown in Fig. 2. In all other cases, the magnetic order is absent. The magnetic moment per nickel atom decreases with an increase in the specific phosphorus content in the system. With increasing pressure, the magnetic moment and magnetic ordering completely disappear at a pressure of 315, 360, 350, and 115 GPa for the $Ni_{14}P$, $Ni_{12}P$, $Ni_{10}P$, and Ni_8P lattices, respectively. Unlike the considered phosphides, the magnitude of the magnetic moment in pure nickel weakly depends on external pressure. With an increase in pressure from 100 to 200 GPa, the magnetic moment per nickel atom decreases from 0.58 μ_B to 0.5 μ_B and then remains practically unchanged.

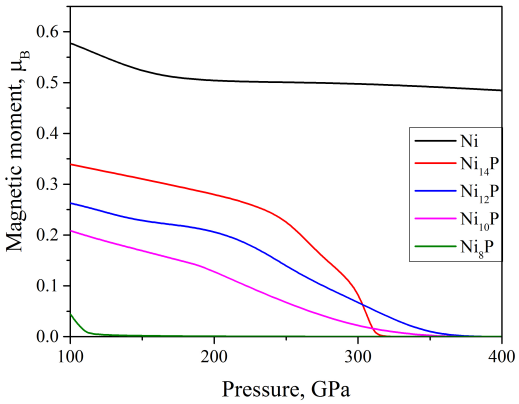

Fig. 2 Pressure dependence of magnatic moment (in Bohr magneton, μ_B) per Ni atom for predicted Ni–P crystal structures. The dependence of the magnetic moment on pressure for pure nickel is given for comparison.

3.2 Thermodynamic of Ni–P compounds

Both sets of the predicted and experimentally observed Ni–P binary compounds were used to evaluate the formation enthalpy ΔH with respect to the elemental solids Ni and P according to Eq. 1, in order to explore the thermodynamic stability of Ni–P:

$$\Delta H(\mathrm{Ni}_n\mathrm{P}_m) = \frac{H(\mathrm{Ni}_n\mathrm{P}_m) - nH(\mathrm{Ni}) - mH(\mathrm{P})}{Z(n+m)}, \qquad (1)$$

where $H = U + PV$ is the entalpy of each compound, Z is a number of structure units in the unit cell and ΔH is the enthalpy of formation per formula unit. Herein, U, P, and V are internal energy, pressure and volume, correspondingly. Detailed information about the element solids can be found in SI.

The relative stabilities of the considered compositions at the selected pressures of 100, 200, 300, and 400 GPa, with ΔH evaluated per atom, are shown in the form of the co-called convex hull Fig. 3, useful for assesing of the phases thermodynamic stability. Points corresponding to the phases with enthalpy lower than the enthalpy of mechanical mixture of the neighbouring compounds forms the convex hull on such a plot. All points above the convex hull corresponds to the unstable phases, which will decompose on the mixture of neighbouring compounds. In addition to predicted and described above $Ni_{14}P$, $Ni_{12}P$, $Ni_{10}P$, Ni_8P, Ni_7P, Ni_5P, Ni_3P, and Ni_2P structures, we have also considered Ni_8P_3 and NiP_2 structures, synthesised experimentally at ambient pressure.

Predicted solid solutions $Ni_{14}P$ – Ni_7P are stable within all pressure range from 100 to 400 GPa, while solid solution enriched with phosphorus are stabilised with pressure. Ni_5P became stable from 200 GPa and above, while Ni_3P from 300 GPa and above. Allabogdanite-NiP_2 is also stabilised against decomposition at 200 GPa. Experimental phase Ni_8P_3 is stable in all pressure range, while NiP_2 destabilised above 300 GPa.

It has to be emphasized, that the results presented in Fig.3 are obtained neglecting thermal effects. In order to account for the effect of temperature on Gibbs energy, we use method of lattice dynamics. Within this method, it is necessary to calculate the vibrational spectra of all the structures considered. We performed phonon mode calculations for all predicted structures, described above. Experimentalyy synthesised Ni_8P_3 was not considered in this context, due to the large size of the unit cell, containing 132 atoms. Speculatively we assume instability of such a low symmetric structure in the filed of high temperatures.

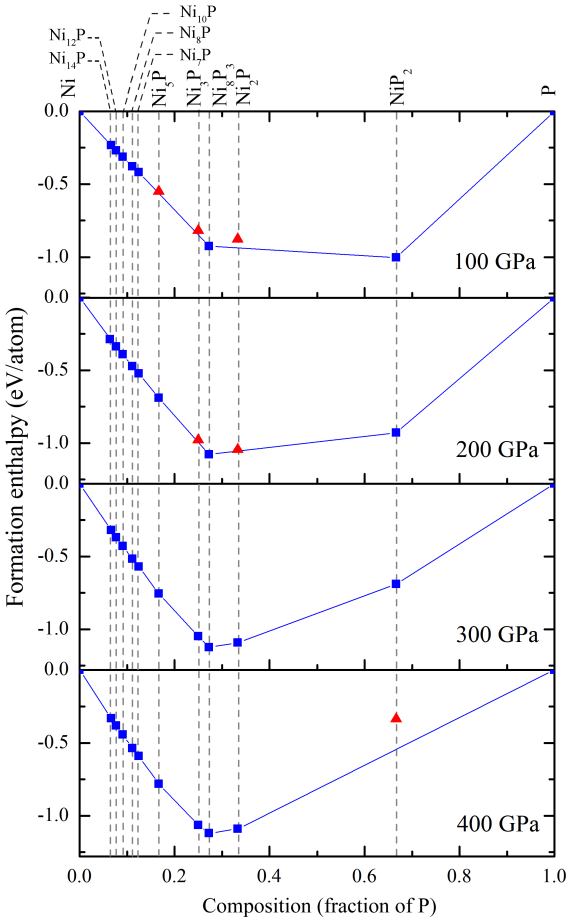

Fig. 3 Convex hulls of Ni–P system at various pressures and 0 K. Blue squares denote stable structures, red triangles - metastable structures. Здесь, как я и говорил выше добавляем схему фазовых переходов

3.2.0.1 PT phase diagrams of Ni_2P and Ni_3P Performed calculations on structure prediction reveal the well-known allabog-

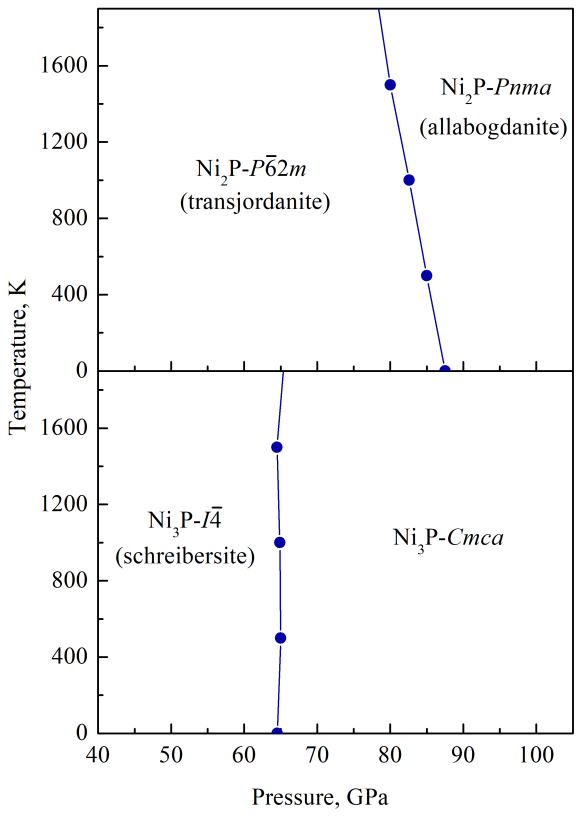

Fig. 4 *P-T* diagram of (a) Ni_2P and (b) Ni_3P. Подписать названия аллабогданит, барринджерит, шрейберзит, цифры сделать строчным шрифтом (не италликом). Слева 'Temperature(K) оставить только один раз посередине'

danite structure of Ni_2P to be the most favorable phase at pressures above 200 GPa. According to experimental data at low pressures, the Ni_2P presents in the form of barringerite structure.[3], and experimental and theoretical studies dis not reveal phase transitions up to 50 GPa.[19,21].

Ni_3P compound at ambient pressure presents in the form of mineral schreibersite, and it's stability was shown up to XXX GPa[2]. In our calculation we reveal another Ni_3P-*Cmca* structure, stable in all investigated pressure range of 100-400 GPa.

Due to natural occurence of schreibersite-Ni_3P, allabogdanite-Ni_2P, and transjordanite-Ni_2P minerals and their findings in metoritic rocks, we determined PT phase diagrams for these compounds within QHA approximation, presented in Fig. 4. The diagrams shows, that transition from barringerite to allabogdanite structure in the Ni_2P system occurs in the pressure range 77-88 GPa at temperatures 0-2000 K. The transition from schreibersite to the found *Cmcm* structure occurs at 62 GPa and pressure of phase transition is almost independent from temperature.

4 Conclusions

Я убрал этот раздел, точнее переместил его в аннотацию. В большинстве журналов он не обязательный, и я уже несколько раз видел рекомендацию "Раздел Выводы необходим только в том случае, если он содержит какую-то дополнительную информацию, не содержащуюся в аннотации".

Acknowledgements

The authors are thankful to the Center for Comput. Mater. Sci., Institute for Materials Research, Tohoku University and Novosibirsk Univesity Supercomputing Center for their continuous support of the supercomputing system to be used for our simulation works.

The reported calculations on crystal structure prediction was funded by RFBR, project number 19-35-90043, calculations of PT diagrams – by the state assignment project of IGM, SBRAS.

References

1 R. Skála and I. Císařová, Physics and Chemistry of Minerals, 2005, 31, 721–732.

2 R. Skála and M. Drábek, Mineralogical Magazine, 2003, 67, 783–792.

3 P. R. Buseck, Science, 1969, 165, 169–171.

4 S. N. Britvin, N. S. Rudashevsky, S. V. Krivovichev, P. C. Burns and Y. S. Polekhovsky, American Mineralogist, 2002, 87, 1245–1249.

5 G. Pratesi, L. Bindi and V. Moggi-Cecchi, American Mineralogist, 2006, 91, 451–454.

6 S. J. B. Reed, Mineralogical Magazine and Journal of the Mineralogical Society, 1968, 36, 850–854.

7 Britvin Sergey N., Shilovskikh Vladimir V., Pagano Renato, Vlasenko Natalia S., Zaitsev Anatoly N., Krzhizhanovskaya Maria G., Lozhkin Maksim S., Zolotarev Andrey A. and Gurzhiy Vladislav V., Scientific Reports, 2019, 9, 1047.

8 S. N. Britvin, M. N. Murashko, Y. Vapnik, Y. S. Polekhovsky, S. V. Krivovichev, O. S. Vereshchagin, N. S. Vlasenko, V. V. Shilovskikh and A. N. Zaitsev, Physics and Chemistry of Minerals, 2019, 46, 361–369.

9 S. N. Britvin, Y. Vapnik, Y. S. Polekhovsky, S. V. Krivovichev, M. G. Krzhizhanovskaya, L. A. Gorelova, O. S. Vereshchagin, V. V. Shilovskikh and A. N. Zaitsev, Mineralogy and Petrology, 2019, 113, 237–248.

10 Britvin Sergey N., Murashko Mikhail N., Vapnik Yevgeny, Polekhovsky Yury S., Krivovichev Sergey V., Vereshchagin Oleg S., Shilovskikh Vladimir V., Vlasenko Natalia S. and Krzhizhanovskaya Maria G., Physics and Chemistry of Minerals, 2020, 47, 3.

11 X. Wu, M. Mookherjee, T. Gu and S. Qin, Geophysical Research Letters, 2011, 38,.

12 H. P. Scott, S. Huggins, M. R. Frank, S. J. Maglio, C. D. Martin, Y. Meng, J. Santillán and Q. Williams, Geophysical Research Letters, 2007, 34,.

13 P. Dera, B. Lavina, L. A. Borkowski, V. B. Prakapenka, S. R. Sutton, M. L. Rivers, R. T. Downs, N. Z. Boctor and C. T. Prewitt, Geophysical Research Letters, 2008, 35,.

14 X. Wu and S. Qin, Journal of Physics: Conference Series, 2010, 215, 012110.
15 T. Gu, X. Wu, S. Qin and L. Dubrovinsky, Physics of the Earth and Planetary Interiors, 2011, 184, 154–159.
16 Z. Zhao, L. Liu, S. Zhang, T. Yu, F. Li and G. Yang, RSC Adv., 2017, 7, 15986–15991.
17 T. Gu, Y. Fei, X. Wu and S. Qin, Earth and Planetary Science Letters, 2014, 390, 296–303.
18 T. Gu, Y. Fei, X. Wu and S. Qin, American Mineralogist, 2016, 101, 205–210.
19 J. Nisar and R. Ahuja, Earth and Planetary Science Letters, 2010, 295, 578–582.
20 P. C. Donohue, T. A. Bither and H. S. Young, Inorganic Chemistry, 1968, 7, 998–1001.
21 P. Dera, B. Lavina, L. A. Borkowski, V. B. Prakapenka, S. R. Sutton, M. L. Rivers, R. T. Downs, N. Z. Boctor and C. T. Prewitt, Journal of Geophysical Research: Solid Earth, 2009, 114,.
22 P. Dera, J. D. Lazarz and B. Lavina, Journal of Solid State Chemistry, 2011, 184, 1997–2003.
23 P. Dera, J. Nisar, R. Ahuja, S. Tkachev and V. B. Prakapenka, Physics and Chemistry of Minerals, 2013, 40, 183–193.
24 K. D. Litasov, A. F. Shatskiy, D. A. Minin, K. E. Kuper and H. Ohfuji, High Pressure Research, 2019, 39, 561–578.
25 J.-S. Chen, C. Yu, H. Lu and J.-M. Chen, Phase Transitions, 2016, 89, 1078–1089.
26 D. Zhao, L. Zhou, Y. Du, A. Wang, Y. Peng, Y. Kong, C. Sha, Y. Ouyang and W. Zhang, Calphad, 2011, 35, 284–291.
27 C. W. Glass, A. R. Oganov and N. Hansen, Computer Physics Communications, 2006, 175, 713–720.
28 A. R. Oganov and C. W. Glass, The Journal of Chemical Physics, 2006, 124, 244704.
29 A. O. Lyakhov, A. R. Oganov and M. Valle, Computer Physics Communications, 2010, 181, 1623–1632.
30 C. J. Pickard and R. J. Needs, Phys. Rev. Lett., 2006, 97, 045504.
31 C. J. Pickard and R. J. Needs, Journal of Physics: Condensed Matter, 2011, 23, 053201.
32 G. Kresse and D. Joubert, Phys. Rev. B, 1999, 59, 1758–1775.
33 G. Kresse and J. Furthmüller, Phys. Rev. B, 1996, 54, 11169–11186.
34 J. P. Perdew, K. Burke and M. Ernzerhof, Phys. Rev. Lett., 1997, 78, 1396–1396.
35 P. E. Blöchl, Phys. Rev. B, 1994, 50, 17953–17979.
36 A. Togo and I. Tanaka, Scripta Materialia, 2015, 108, 1–5.
37 P. N. Gavryushkin, K. D. Litasov, S. S. Dobrosmislov and Z. I. Popov, physica status solidi (b), 2017, 254, 1600857.
38 P. N. Gavryushkin, Z. I. Popov, K. D. Litasov, A. B. Belonoshko and A. Gavryushkin, Geophysical Research Letters, 2016, 43, 8435–8440.
39 S. Oryshchyn, V. Babizhetskyy, S. Chykhriy, L. Aksel'rud, S. Stoyko, I. Bauer, R. Guerin and Y. Kuz'ma, Inorganic Materials, 2004, 40, 380–385.